33. D. Bercovici, *Earth Planet. Sci. Lett.* **144**, 41 (1996).
34. S. A. Weinstein, *Earth Planet. Sci. Lett.* **155**, 87 (1998).
35. P. J. Tackley, *Earth Planet. Sci. Lett.* **157**, 9 (1998).
36. R. Trompert and U. Hansen, *Nature* **395**, 686 (1998).
37. P. J. Tackley, *Geochem. Geophys. Geosyst.*, in press.
38. ———, *Geochem. Geophys. Geosyst.*, in press.
39. K. Regenauer-Lieb and D. A. Yuen, *Geophys. Res. Lett.* **25**, 2737 (1998).
40. J. Braun *et al.*, *J. Geophys. Res.* **104**, 25167 (1999).
41. M. Kameyama, D. A. Yuen, H. Fujimoto, *Geophys. Res. Lett.* **24**, 2523 (1997).
42. A. M. Hofmeister, *Science* **283**, 1699 (1999).
43. D. Bercovici, Y. Ricard, G. Schubert, in preparation.
44. M. Yoshida, Y. Iwase, S. Honda, *Geophys. Res. Lett.* **26**, 947 (1999).
45. J. P. Lowman and G. T. Jarvis, *J. Geophys. Res.* **101**, 25485 (1996).
46. M. Gurnis, *Nature* **332**, 695 (1988).
47. J. P. Lowman and G. T. Jarvis, *J. Geophys. Res.* **104**, 12773 (1999).
48. A. Lenardic and W. M. Kaula, *Nature* **378**, 709 (1995).
49. A. Lenardic, *Geophys. J. Int.* **134**, 706 (1998).
50. ——— and L.-N. Moresi, *J. Geophys. Res.* **104**, 12747 (1999).
51. S. S. Shapiro, B. H. Hager, T. H. Jordan, *Lithos* **48**, 115 (1999).
52. M. P. Doin, L. Fleitout, U. Christensen, *J. Geophys. Res.* **102**, 2771 (1997).
53. Incompatible trace elements are present in small concentrations and are not readily incorporated into silicate crystal lattices, and thus tend to enter any melt that forms.
54. This depletion is relative to a "primitive" composition, which is the presumed composition of Earth's mantle before the extraction of any continental crust.
55. A seismic discontinuity at 660 km depth, which is now understood to result from a phase transition, separates the upper and lower mantles.
56. R. D. van der Hilst, S. Widiyantoro, E. R. Engdahl, *Nature* **386**, 578 (1997).
57. S. P. Grand, R. D. van der Hilst, S. Widiyantoro, *GSA Today* **7**, 1 (1997).
58. G. Masters, G. Laske, H. Bolton, A. Dziewonski, in *Mineral Physics and Seismic Tomography*, S. Karato *et al.*, Eds. (American Geophysical Union, Washington, DC, 2000), pp. 63–87.
59. Both a viscosity increase and a deflection of the phase boundary within upwellings and downwellings may temporarily deflect slabs.
60. P. J. Tackley, *U.S. National Report to the IUGG 1991–1994* (American Geophysical Union, Washington, DC, 1985), pp. 275–282.
61. U. R. Christensen, *Earth Planet. Sci. Lett.* **140**, 27 (1996).
62. ———, *J. Geophys. Res.* **102**, 22435 (1997).
63. M. Gurnis and G. F. Davies, *Geophys. Res. Lett.* **13**, 541 (1986).
64. P. E. van Keken and C. J. Ballentine, *Earth Planet. Sci. Lett.* **156**, 19 (1998).
65. ———, *J. Geophys. Res.* **104**, 7137 (1999).
66. S. Ferrachat and Y. Ricard, *Earth Planet. Sci. Lett.* **155**, 75 (1998).
67. Possible regimes of mixing are chaotic (turbulent), in which stretching of heterogeneities increases exponentially with time, and laminar, in which stretching increases linearly with time. Steady-state flows without toroidal motion exhibit only laminar mixing.
68. P. E. van Keken and S. Zhong, *Earth Planet. Sci. Lett.* **171**, 533 (1999).
69. A. A. Ten, Y. Y. Podladchikov, D. A. Yuen, T. B. Larsen, A. V. Malevsky, *Geophys. Res. Lett.* **25**, 3205 (1998).
70. M. Manga, *Geophys. Res. Lett.* **23**, 403 (1996).
71. T. W. Becker, J. B. Kellogg, R. J. O'Connell, *Earth Planet. Sci. Lett.* **171**, 351 (1999).
72. T. Lay, Q. Williams, E. J. Garnero, *Nature* **392**, 461 (1998).
73. I. Sidorin, M. Gurnis, D. V. Helmberger, *J. Geophys. Res.* **104**, 15005 (1999).
74. X.-F. Liu, J. Tromp, A. M. Dziewonski, *Earth Planet. Sci. Lett.* **160**, 343 (1998).
75. J. Ritsema, S. Ni, D. V. Helmberger, H. P. Crotwell, *Geophys. Res. Lett.* **25**, 4245 (1998).
76. D. A. Yuen, O. Cadek, A. Chopelas, C. Matyska, *Geophys. Res. Lett.* **20**, 899 (1993).
77. P. F. Thompson and P. J. Tackley, *Geophys. Res. Lett.* **25**, 1999 (1998).
78. M. Ishii and J. Tromp, *Science* **285**, 1231 (1999).
79. W.-J. Su and A. M. Dziewonski, *Phys. Earth Planet. Inter.* **100**, 135 (1997).
80. B. L. N. Kennett, S. Widiyantoro, R. D. van der Hilst, *J. Geophys. Res.* **103**, 12469 (1998).
81. P. J. Tackley, D. J. Stevenson, G. A. Glatzmaier, G. Schubert, *J. Geophys. Res.* **99**, 15877 (1994).
82. U. R. Christensen and A. W. Hofmann, *J. Geophys. Res.* **99**, 19867 (1994).
83. F. Albarade, *Chem. Geol.* **145**, 413 (1998).
84. N. Coltice and Y. Ricard, *Earth Planet. Sci. Lett.* **174**, 125 (1999).
85. P. J. Tackley, in *The Core-Mantle Boundary Region*, M. Gurnis, M. E. Wysession, E. Knittle, B. A. Buffett, Eds. (American Geophysical Union, Washington, DC, 1998), pp. 231–253.
86. L. H. Kellogg, B. H. Hager, R. D. van der Hilst, *Science* **283**, 1881 (1999).
87. C. Lithgow-Bertelloni and P. G. Silver, *Nature* **395**, 269 (1998).
88. A. M. Forte, J. X. Mitrovica, R. L. Woodward, *Geophys. Res. Lett.* **22**, 1013 (1995).
89. R. D. van der Hilst and H. Karason, *Science* **283**, 1885 (1999).
90. A. Davaille, *Nature* **402**, 756 (1999).
91. I thank J. Vidale for suggesting Fig. 2B, and two anonymous reviewers for helpful advice. Supported by NASA and the David and Lucile Packard Foundation.

REVIEW

Earth's Core and the Geodynamo

Bruce A. Buffett

Earth's magnetic field is generated by fluid motion in the liquid iron core. Details of how this occurs are now emerging from numerical simulations that achieve a self-sustaining magnetic field. Early results predict a dominant dipole field outside the core, and some models even reproduce magnetic reversals. The simulations also show how different patterns of flow can produce similar external fields. Efforts to distinguish between the various possibilities appeal to observations of the time-dependent behavior of the field. Important constraints will come from geological records of the magnetic field in the past.

Earth evolved into a layered body early in its history. Molten metal (mainly iron) descended to form the present-day core, while silicates and oxides were confined to a thick shell called the mantle. The innermost part of the core is now solid, whereas the outer portion is liquid (Fig. 1). The viscosity of the liquid outer core is comparable to that of water (*1*), which permits vigorous convection as the core cools. Fluid velocities on the order of 10 km per year, (*2*) are sufficiently rapid to sustain Earth's magnetic field through a mechanism known as the geodynamo.

Department of Earth and Ocean Sciences, University of British Columbia, 2219 Main Mall, Vancouver, BC, Canada V6T 1Z4. E-mail: buffett@eos.ubc.ca

Planetary rotation promotes the types of flows that are needed to generate the magnetic field. However, the resulting magnetic field exerts a strong feedback on convection, which complicates quantitative predictions of the field generation. An important advance in recent years is the development of numerical simulations that achieve self-sustaining dynamo action (*3–5*). Computational limitations prevent these simulations from reaching Earth-like conditions, but the models obtained so far have external magnetic fields that are similar to Earth's field (Fig. 2).

The operation of the geodynamo depends on the internal evolution of the planet because convection in the core is linked to the rate of cooling. The transport of heat through the mantle is crucial for powering the geodynamo, and even the existence of plate tectonics at the surface is an important factor. Interactions between the core and the mantle are expected, though it is unclear how these interactions are expressed in the magnetic field. Persistence of the magnetic field over most of Earth's history implies continual cooling and convection in the core. By contrast, the absence of magnetic fields in our nearest planetary neighbors (*6*) indicates that other thermal histories are possible. As we gain a better understanding of the geodynamo and the dynamics of the core, new perspectives about the processes that drive the internal evolution of Earth are expected to emerge (*7*).

Origin and Evolution of the Core

The initial supply of energy for the geodynamo is established by the state of the core at the time of its formation (*8*). Subsequent cooling delivers this energy to the geodynamo over geological time. Although a detailed reconstruction of the formation and evolution of the core is not possible, we can identify some of the processes that must have occurred. It is generally believed that the core began forming soon after Earth started to accrete from the solar nebula (*9*). The heat produced by impacts during accretion was probably sufficient to cause large-scale, and possibly complete, melting of the planet (*10*). Molten metallic iron would have separated from the surrounding mixture of silicates and oxides to form a dense liquid that sank to the center.

Separation of Earth into a liquid iron core and crystalline mantle represents global change on a colossal scale. The descent of liquid iron into the center of Earth released enough gravitational energy to warm the planet by several thousand degrees (*11*). Metals such as Ni and Co were preferentially extracted from the starting matrix of material and were transported with the liquid iron into the core (*12*). Heavy heat-producing elements, such as U and Th, were probably left behind in the mantle. Questions about heat-producing isotopes in the core usually focus on the fate of K. Experiments at moderate pressure suggest that the solubility of K in liquid iron is too low to deliver a significant amount of the radioactive isotope ^{40}K to the core (*13*). However, theoretical calculations (*14*) suggest that K behaves like a transition metal at high pressure and may become much more soluble in iron at depth. Unfortunately, the partitioning of K into liquid iron depends on a number of other factors (*15*). Current uncertainties prevent a definitive assessment of the radioactive heat sources in the core.

Few observations are available to constrain the composition of the core. Seismology provides an estimate of the radial density profile in the liquid core (*16*), which is typically 10% lower than the density of pure iron (*17*). Light alloying elements are required to explain the density deficit, but the identity of the major light element(s) is presently unknown. Arguments for and against commonly cited elements, including H, C, O, S, and Si, depend on local thermodynamic conditions where iron melts or subsequently equilibrates with the silicate mantle (*18*). The observed profiles of density and bulk modulus make few distinctions between the proposed light elements (*19*).

Estimates of density in the solid inner core are consistent with pure iron, though small amounts of light elements may be present (*20*). This conclusion is supported by recent theoretical calculations of the density of solid iron at high pressure and temperature (*21*). The predicted density is about 2 to 3% greater than the seismic estimates, suggesting that light elements are present at low concentrations compared with the liquid core (*22*, *23*). Theoretical estimates of the liquid properties of iron at high pressure and temperature (*23*) indicate that about 30% of the density change at the inner-core boundary is attributed to the volume change on solidification. The remainder is probably due to a change in the concentration of light elements across the inner-core boundary.

The exclusion of light elements from the inner core provides an important source of buoyancy for convection (*24*). Light elements rise into the fluid outer core, while denser elements solidify into the inner core. Thermal buoyancy may also be important, but the role of thermal convection in the core is complicated by the influence of the mantle (*25*, *26*). The more massive and relatively sluggish mantle controls the cooling of the core by regulating the heat flow across the core-mantle boundary. Restrictions on the rate of cooling are important because of the high thermal conductivity of liquid iron. The heat carried by conduction along the average temperature gradient through the core can be comparable to the total heat flow into the base of the mantle. Because the conducted heat flow does not contribute to convection, it is only the excess heat flow that is important from the point of view of magnetic-field generation. Uncertainties in the value of the heat flow at the base of the mantle permit a wide range of possibilities for the strength of thermal convection. Some estimates even sugest that the conducted heat flow exceeds the heat flow into the base of the mantle (*27*). Under these circumstances, heat must be convectively mixed down into the core by compositional convection, diverting power from the geodynamo (*28*); otherwise, a warm layer will develop at the top of the core (*29*).

Convection in the core operates as a giant heat engine. Heat is drawn from the core by the mantle and work is done to maintain the magnetic field. The sources of thermal and compositional buoyancy are connected by the thermal evolution of the core. Cooling the core causes solidification of the liquid iron and, hence, growth of the inner core. The fractionation of light elements into the outer core lowers the gravitational energy. Most of this rearrangement occurs by convection, so the release of gravitational energy is available to power the geodynamo (*30*). Latent heat release and cooling can also power the geodynamo,

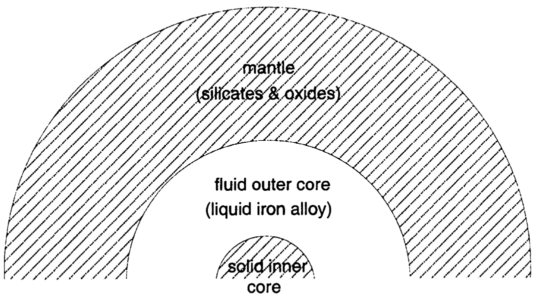

Fig. 1. Schematic view of Earth's primary layered structure. The iron core is divided into a solid inner core and a fluid outer core. The overlying mantle is composed of silicates and oxides. Cooling of the core causes growth of the inner core by solidification. The current rate of growth is about 1 mm per year. Fractionation of light alloying elements into the fluid outer core provides an important source of buoyancy for driving convection.

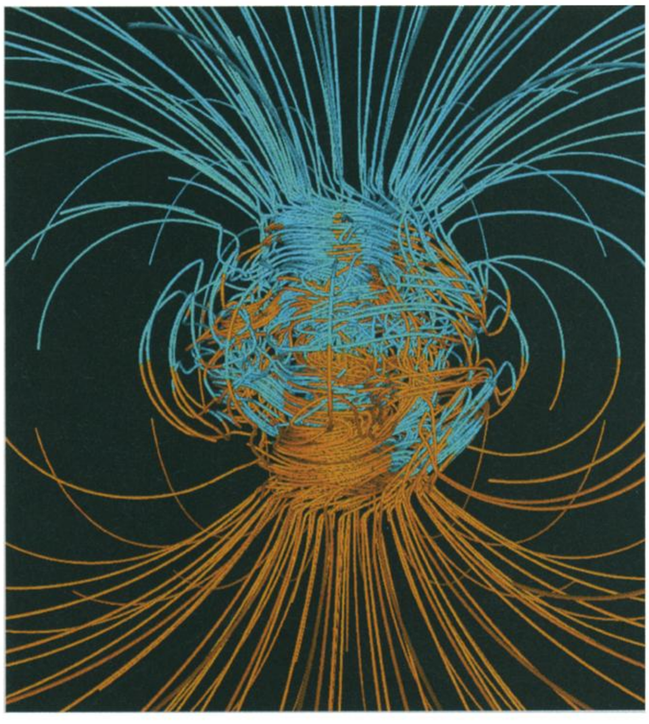

Fig. 2. Three-dimensional structure of the magnetic field at one time-step from the Glatzmaier-Robert geodynamo model (3). The field has a complicated form inside the core but exhibits a nearly dipole structure outside the core. Yellow and blue are used to distinguish the field lines that are directed into and out of the core, respectively. A dominant feature in the interior is defined by the field lines that are wrapped by flow to form a cylinder. This structure coincides with the surface of the tangent cylinder.

but only if the total heat flow exceeds the heat conducted across the core.

In the spirit of the heat engine analogy, it is possible to define Carnot efficiencies that describe the importance of thermal and compositional convection in the geodynamo problem (*31*). The estimates are subject to large uncertainties, but compositional convection probably contributes about 80% of the power to the geodynamo and thermal convection about 20%. At earlier times, compositional convection should have been weaker because the inner core was smaller. Before the formation of the inner core, convection would have been driven entirely by thermal convection. Plausible thermal histories indicate that the inner core formed about 2 billion years ago (Ga) (*26*, *29*, *32*). If this is true, then the operation of the geodynamo before this time would depend on the viability of thermal convection. Evidence that the magnetic field was present 3.5 Ga (*33*) suggests that cooling was rapid enough to sustain vigorous thermal convection (*32*).

Generation of the Magnetic Field

Persistence of the magnetic field over geological time requires continual regeneration because ohmic losses can dissipate the field in about 10^4 years (*34*). Convective velocities in Earth's core are thought to be sufficient to overcome these ohmic losses. Planetary rotation causes spiraling convective flows that align with the rotation axis (*35*). The magnetic field is amplified by these helical motions through a mechanism known as the α effect (Fig. 3). Zonal flows may also be present, which produce large rates of shear across the outer core and provide another mechanism for generating the magnetic field; this mechanism is often called the ω effect. Different styles of dynamo action can be characterized on the basis of the relative importance of the α and ω effects (*36*). The so-called $\alpha\omega$ dynamo relies on a combination of helical and zonal flows, whereas the α^2 dynamo relies entirely on the helical flows. Both $\alpha\omega$ and α^2 dynamos have been produced in recent numerical simulations.

The columnar pattern of convection can be understood as a consequence of the well-known Taylor-Proudman condition, which applies to rapidly rotating fluids (*37*). The fluid velocity $\mathbf{v}$ in a frame rotating with angular velocity $\boldsymbol{\Omega}$ is governed approximately by a balance between the Coriolis force and the pressure gradient

$$2\rho\boldsymbol{\Omega}\times\mathbf{v} = -\nabla P \tag{1}$$

where P is the fluid pressure, ρ is the density, and ∇ is the usual gradient operator. [Horizontal flow in the atmosphere is governed by the same equation to a first approximation (*38*). Such fluid motion is known as geostrophic flow.] In a constant density fluid, the curl of the geostrophic force balance yields the Taylor-Proudman condition, $(\boldsymbol{\Omega}\cdot\nabla)\mathbf{v} = 0$, which means that motion does not vary in the direction of the rotation axis. In a contained fluid like the core, this implies that the component of velocity along the rotation axis vanishes. The fluid is constrained to circulate around the core along streamlines that coincide with lines of latitude.

Convection entails departures from a purely geostrophic force balance. In addition to buoyancy forces, convection in a rapidly rotating fluid requires viscous and/or magnetic (Lorentz) forces in the force balance (*39*). Because of the low viscosity of liquid iron, viscous forces are not important unless the length scale of the flow is less than 10^2 m (*40*). Alternatively, Lorentz forces become important when the magnetic field exceeds 10^{-3} T (*41*). These two possibilities result in very different styles of convection. Dynamos that sustain a magnetic field less than 10^{-3} T are associated with small-scale convection and are known as weak-field dynamos. However, once the magnetic field exceeds 10^{-3} T, Lorentz forces play a leading role and convection becomes large-scale (e.g., comparable to the radius of the core). These dynamos are called strong-field dynamos. Because weak-field dynamos are expected to be unstable as the vigor of convection increases (*36*), the geodynamo probably operates in the strong-field regime. A recent convection calculation with an imposed magnetic field (*42*) shows that strong-field solutions can also be unstable to changes in the configuration of the imposed field. If these conditions are applicable to Earth, the calculations suggest that the geodynamo may revert to a weak-field state, at least temporarily. Observations of disruptions in the field every 30,000 to 100,000 years have been attributed to this temporary transition (*43*).

Perhaps the most important advance in the past few years is the development of numerical simulations that achieve self-sustaining dynamo action (*3–5*). No prior form is imposed on either the magnetic or velocity fields. Instead, both fields are free to evolve in response to the flow of heat and/or light

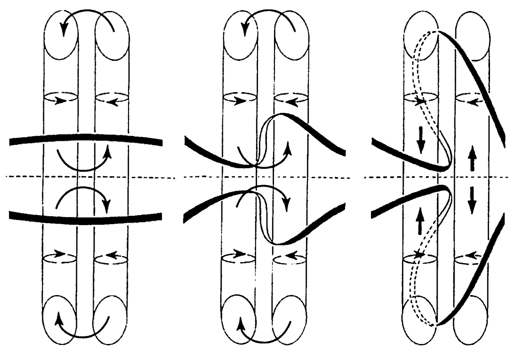

Fig. 3. Schematic illustration of the α effect from the study of Olson, Christensen, and Glatzmaier [in (*5*), copyright by the American Geophysical Union]. Helical flows are organized into columns that extend across the core in the direction of the rotation axis. Arrows indicate the direction of flow. An initially zonal magnetic field (left) is represented by two thick lines on either side of the equator (dashed line). The helical flow distorts the initial field configuration to produce loops of field that are perpendicular to the initial field (right). An analogous mechanism operates on an initially vertical magnetic field.

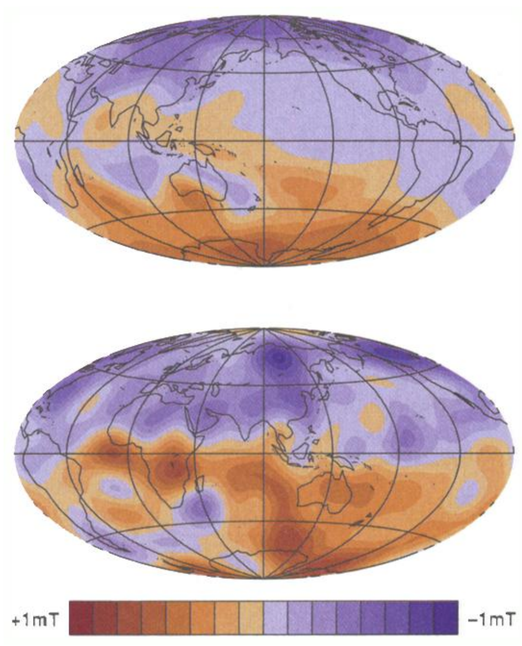

Fig. 4. Comparison of (top) the radial magnetic field predicted by the Kuang-Bloxham dynamo model (*4*) at the core-mantle boundary and (bottom) the observed radial magnetic field (continued to the core-mantle boundary, assuming that the mantle is an electrical insulator). Both the predicted and observed fields have a dominant dipole component, but nondipole features are also evident. In the observed field, strong patches are evident below Siberia and south of Australia. Somewhat weaker field is observed directly below the polar regions.

elements at the boundaries. Interactions between convection and magnetic field generation strongly influence the time-averaged form of the resulting magnetic and velocity fields and may permit multiple solutions to exist. Computational limitations currently prevent these calculations from reaching Earth-like physical conditions, but the models still produce external fields with a dominant dipole component (Fig. 4).

Some of the computational difficulties that are encountered in the numerical simulations arise in trying to account for inertial and viscous forces, which are small compared with leading-order terms like the Coriolis force. The ratio of the viscous force to the Coriolis force defines the Ekman number, E, which is nominally 10^{-15}. Turbulence in the core increases the effective viscosity, but physical considerations (*44*) suggest that E remains small (e.g., $E \approx 10^{-9}$). The ratio of the Rossby number (Ro) of the inertial force (in the rotating frame) to the Coriolis force is 10^{-7} for fluid velocities on the order of 10 km year^{-1}. Attempts to neglect the inertial and viscous effects have not been successful (*45*), but it is not computationally feasible to retain these terms with Earth-like values. Different strategies have been adopted in the recent numerical simulations to approximate the conditions in the Earth.

The approach used by Glatzmaier and Roberts (*3*) is to make the effects of viscosity and inertia as small as possible. Their initial calculations produced strong-field dynamos using $Ro = 0$ and $E = 2 \times 10^{-6}$, whereas subsequent calculations (*46*) restored the axisymmetric part of the inertial force. Fluid motion in their calculations is largely confined to a cylinder that encloses the inner core (e.g., the tangent cylinder). Dynamo action occurs inside the tangent cylinder through a combination of zonal and helical flows. Upwelling along the rotation axis causes divergence of flow at the core-mantle boundary and a westward circulation by conservation of angular momentum. At the inner-core boundary, a convergent flow produces an eastward circulation, which is coupled to the inner core by magnetic stresses. Because the inner core is free to rotate, the overriding flow sweeps the inner core in an eastward direction (*47*). The predicted rate of rotation varied in these calculations, but the average value was about 2° per year (*48*). More recent calculations using a higher spatial resolution and no hyperviscosity predict a rotation rate of 0.17° per year (*49*).

An alternative strategy is adopted in the model of Kuang and Bloxham (*4*). They reduced the influences of viscous forces at the boundaries by using stress-free boundary conditions, rather than the more commonly used no-slip conditions. Viscous forces are retained in the interior of the core, and the axisymmetric part of the inertial force is also included. Some features of their strong-field solutions using $Ro = E = 2 \times 10^{-5}$ are similar to those of Glatzmaier and Roberts. Both solutions produce a dominant dipole field at the core-mantle boundary, and the generation mechanisms both rely on a combination of helical and zonal flows (e.g., $\alpha\omega$ dynamos). However, the most vigorous dynamo action in the Kuang-Bloxham dynamo occurs outside the tangent cylinder, which is opposite to the predictions of the Glatzmaier-Roberts dynamo. Part of the difference is attributed to the choice of stress-free versus no-slip conditions, which indicates that viscous forces at the boundaries of the core play an important role in the numerical simulations, even when E is 10^{-5}.

Some ambiguity arises in the interpretation of E in these simulations because of the nonstandard treatment of the viscous force. In order to construct a stable numerical scheme, the viscous force is replaced by one that enhances the damping of flow as the length scale decreases. Although turbulent diffusivities are commonly used in numerical models, there is little physical basis for making the effective diffusivity dependent on the length scale of the flow. Concerns about the influence of this form of diffusion on numerical simulations (*50*) have motivated new studies that use constant turbulent diffusivities. Solutions with constant diffusivity have been obtained where E ranges from 10^{-3} to 10^{-4} (*5*).

All of these recent simulations predict columnar convection outside the tangent cylinder. The magnetic fields are generated primarily by helical flows with relatively little contribution from zonal flows (e.g., α^2 dynamos). The resulting field at the core-mantle boundary has a dominant dipole component (*51*), but it also exhibits nondipole features that are similar to those observed in Earth's field (Fig. 4). In particular, patches of strong field are predicted at high latitudes, where convergent motions sweep the field into regions of downwelling. Indeed, the superposition of these patches is responsible for the dipole component in the simulations. These calculations also predict a weak field in the polar regions due to divergence of flow, supporting earlier speculations about the origin of this feature in Earth's field (*52*). Although these simulations are still far from Earth-like conditions, the predictions show encouraging similarities with the present-day structure of Earth's field.

A complementary source of information comes from observations of the long-term behavior of the magnetic field. The direction and intensity of the magnetic field in the past can be inferred from the magnetization acquired by rocks at the time of their formation. Changes in this fossil magnetism over time reveal that the magnetic field has reversed polarity at irregular intervals in the past (*53*). Estimates have also been obtained for the variability in the apparent direction of the dipole field during periods of stable polarity. Evidence of long-period trends in these data has often been interpreted as indications of an external influence of the mantle on the core (*54*). Geodynamo models now offer a more quantitative means of testing these speculations.

External Influences on the Geodynamo

Processes associated with the geodynamo occur on time scales that are relatively short in geological terms. Magnetic waves are expected to have periods of 10 to 10^2 years (*55*), whereas convection carries fluid through the core in about 10^3 years. Ohmic losses can dissipate the magnetic in 10^4 years, and magnetic reversals occur with an average recurrence interval of about 10^5 years during the recent geological past (*53*). Evidence of much slower processes in the core is usually attributed to an external influence from the mantle. One example is the gradual change in the average reversal frequency over periods of 10^8 years, which is much more characteristic of time scales for convection in the mantle (*54*). Another example involves the nondipole features in the magnetic field that have persisted for millions of years at the same location relative to the mantle (*56*). These features suggest that the generation of magnetic field is tied in some way to lateral heterogeneity at the base of the mantle. However, it is not clear how the mantle exerts its influence on the core.

Various sources of interaction can arise from lateral heterogeneity in the lowermost mantle (*57*). Thermal interactions are one possibility that may result from convection in the mantle (*54*, *58*). Temperature anomalies of a few hundred degrees near the base of the mantle should cause large variations in heat flow across the surface of the core-mantle boundary. Fluid motion induced at the top of the core interferes with the deeper convective circulation. Some numerical calculations indicate that the pattern of convection in the core becomes locked to the imposed pattern of heat flow (*59*), whereas other calculations predict greater variability in the pattern of flow (*60*). Laboratory experiments offer further evidence of complexity (*61*).

Geodynamo simulations have only recently explored the consequences of variations in heat flow at the core-mantle boundary. Simulations using the Glatzmaier-Roberts dynamo show that changes in the pattern of heat flow at the core-mantle boundary can alter the frequency of reversals, depending on the imposed pattern of heterogeneity (*62*). These simulations also show that heat-flow conditions influence the temporal variability of the field during intervals of stable polarity. Simulations using the Kuang-Bloxham dynamo model find that better agreement between the predicted and observed variability is achieved when lateral variations in heat flow are included in the model (*63*). Particular choices of heat-flow conditions also appear to enhance nondipole features in the field (*64*).

Other interactions can arise from variations in electrical conductivity at the base of the mantle (*65*). Electric currents from the core flow along conductive pathways through the mantle. Magnetic induction associated with this electric current can contribute to the external magnetic field (*66*). Calculations suggest that the induced field may be large enough to account for the stationary features in the field (*67*). Variations in electrical conductivity may also contribute to the exchange of angular momentum between the core and the mantle (*68*), which would have observable consequences for Earth's rotation. Regions of anomalous electrical conductivity may correlate with anomalous thermal conductivity, thereby altering heat flow from the core (*69*).

Still other types of interaction can result from gravitational attraction between mass, which is distributed heterogeneously through the core and the mantle (*70*). Topographic variations in the core-mantle boundary can deflect flow at the top of the core and disturb the magnetic field in the interior (*71*). The importance of these potential interactions is not yet understood.

Surprises in the Inner Core

Growing evidence of elastic anisotropy in the inner core continues to yield surprises. Elastic anisotopy was first proposed 15 years ago, when it appeared that seismic waves traveled several percent faster along polar paths through the inner core than along equatorial paths (*72*). The picture has become increasingly complicated as more observations have been collected (*73*). There is evidence of three-dimensional variations in the anisotropy at scales ranging from 10^3 m to 10^6 m (*74*). There are also indications that the anisotropy is weak or absent in the outermost few hundred kilometers of the inner core (*75*).

Appreciable anisotropy in the inner core is difficult to explain. First, a high degree of crystal alignment in the inner core is required to explain the seismic observations. Alignments of 30 to 100% of the crystals have been suggested on the basis of predicted elastic properties of iron at high pressure (*23*, *76*). Alternative explanations that involve melt-filled inclusions (*77*) appear to have similar difficulties because viscous compaction should gradually close the inclusions and expel the fluid (*78*). Second, there is no clear understanding of how a preferential alignment develops. Although a number of mechanisms have been proposed (*79*), none of these are entirely satisfactory (*80*). Efforts to find more viable explanations continue in the hope that a better understanding of the elastic anisotropy will offer new clues about the evolution of the core.

Several recent studies have used the existence of longitudinal variations in elastic anisotropy to infer that the inner core rotates faster than the mantle. The detection of this relative rotation is based on systematic changes in the travel time of seismic waves over the past 30 years. The measured changes in travel time are related to a rate of inner-core rotation by assuming a model for lateral variations in elastic properties in the inner core. Two initial studies (*81*) obtained rotation rates of 1° to 3° per year with a cylindrical model of elastic anisotropy with a symmetry axis inclined to the rotation axis (*82*). Lower rates of 0.2° to 0.3° per year were reported in a subsequent study (*83*) that used similar data but adopted a regional elastic model with steeper gradients in anisotropy.

More recent studies using different travel-time measurements (*84*) or normal-mode observations (*85*) find no evidence of relative rotation with an uncertainty as low as ±0.2° per year. It is possible that gravitational interactions between the inner core and the mantle prevent relative rotation (*86*). It is also possible that relative rotation occurs at a rate that is below current detection. High-quality seismic data continue to accumulate, though bounds on the allowable rotation rate will not change greatly in the next few years. More progress can be made in the short term by analyzing older records of earthquakes in the hope of extending the observational evidence back to the 1950s or earlier (*87*).

Future Prospects

Continuing advances in computing capabilities will inevitably improve models of the geodynamo. Greater spatial resolution and longer integrations will reduce some of the difficulties that are presently encountered. However, future progress will not rely solely on incremental advances in computing capabilities. A better understanding of turbulence in the core and its influence on the resolvable part of the flow will be essential for improving the reliability of geodynamo simulations. Present schemes that account for turbulence with isotropic diffusivities may not be adequate because the effect of rotation and magnetic field can make turbulence strongly anisotropic (*44*). A potentially more serious limitation is that turbulent diffusivities only account for the transfer of energy from large scales to small scales. More effort will be required to reliably describe the turbulent interactions that transfer magnetic energy back to the large scales.

Demands for more realistic simulations will be driven by the desire to compare theoretical predictions with observations. Existing simulations offer tantalizing clues about the origin of magnetic field, but these insights are qualified by questions about the approximations used in the geodynamo models. Innovative comparisons between observations and geodynamo predictions will be critical for guiding future improvements, principally by identifying shortcomings in the predictions.

Geodynamo models will continue to open new opportunities for studying interactions between the core and the rest of Earth. Thermal interactions with the mantle may prove to be the most important. Estimates of the heat flow across the core-mantle boundary influence the vigor of thermal convection in the core and control the growth rate of the inner core. These influences should be reflected in the magnetic field. A better understanding of these influences will allow their signature in paleomagnetic observations to be interpreted. Even the sustained operation of the geodynamo over geological time is an important distinction between the internal evolution of Earth and that of Venus or Mars.

References and Notes

1. Theoretical calculations for liquid iron at the physical conditions of Earth's core predict a viscosity of $\mu = 10^{-2}$ Pa s [G. A. de Wijs *et al.*, *Nature*, **392**, 805 (1998)]. The kinematic viscosity $\nu = \mu/\rho$ of iron, where ρ is the fluid density, is comparable to the value for water.
2. Fluid velocities at the top of the core are inferred from time variations in the magnetic field. A review of the theory and observations is given by J. Bloxham and A. Jackson [*Rev. Geophys.* **29**, 97 (1991)].
3. G. A. Glatzmaier and P. H. Roberts, *Phys. Earth Planet. Inter.* **91**, 63 (1995).
4. W. Kuang and J. Bloxham, *Nature* **389**, 371 (1997).
5. A. Kageyama and T. Sato, *Phys. Rev. E* **55**, 4617 (1998); A. Sakuraba and M. Kono, *Phys. Earth Planet. Inter.* **111**, 105 (1998); P. Olson, U. Christensen, G. A. Glatzmaier, *J. Geophys. Res.* **104**, 10383 (1999); E. Grote, F. H. Busse, A. Tilgner, *Phys. Earth Planet. Inter.* **117**, 259 (2000).
6. Detection of magnetized rocks in ancient parts of the crust on Mars indicate that the planet once had a magnetic field. The absence of magnetization in younger rocks suggests that the internal dynamo ceased early in the history of Mars [M. H. Acuna *et al.*, *Science* **284**, 794 (1999)]. There is no evidence of a magnetic field on Venus at the present time and its surface temperature is too high to preserve a record of a former magnetic field [C. T. Russell, *J. Geophys. Res.* **98**, 18681 (1993)].
7. D. J. Stevenson, *Science* **287**, 997 (2000).
8. D. Gubbins, T. G. Masters, J. A. Jacobs, *Geophys. J. R. Astron. Soc.* **59**, 57 (1979).
9. Constraints on the timing of core formation are derived from radioisotopic dating methods. Early studies relied on measurements of Pb isotopes [X. Overby and X. Ringwood, *Nature* **234**, 463 (1971)], whereas more recent work has focused on the products of short-lived radionuclides. Interpretation of tungsten isotopes suggest that core formation was effectively completed 60 million years after the start of accretion [A. N. Halliday and D. C. Lee, *Geochim. Cosmochim. Acta* **63**, 4157 (1999)].
10. E. Pierazzo, A. M. Vickery, H. J. Melosh, *Icarus* **127**, 408 (1997).
11. F. M. Flasar and F. Birch, *J. Geophys. Res.* **78**, 6101 (1973).
12. O. Tschauner *et al.*, *Nature* **398**, 604 (1999).
13. N. L. Chabot and M. J. Drake, *Earth Planet. Sci. Lett.* **173**, 361 (1999).
14. L. J. Parker, T. Atou, J. V. Badding, *Science* **273**, 95 (1996).

15. K. Righter, M. J. Drake, G. Yaxley, *Phys. Earth Planet. Inter.* **100**, 115 (1997).
16. B. L. N. Kennett, *Geophys. J. Int.* **132**, 374 (1998).
17. R. G. McQueen and S. P. Marsh, *J. Geophys. Res.* **71**, 1751 (1966).
18. J.-P. Poirier, *Phys. Earth Planet Sci.* **85**, 319 (1994).
19. Q. Williams and E. Knittle, *Phys. Earth Planet. Inter.* **100**, 49 (1997).
20. A. Jephcoat and P. Olson, *Nature* **325**, 332 (1987).
21. The stable phase of iron at pressure and temperature conditions of the inner core is thought to be a hexagonal close-packed structure [L. Stixrude and R. E. Cohen, *Geophys. Res. Lett.* **22**, 125 (1997)].
22. L. Stixrude, E. Wasserman, R. E. Cohen, *J. Geophys. Res.* **102**, 24729 (1997).
23. A. Laio *et al.*, *Science* **287** 1027 (2000).
24. S. I. Braginsky, *Dokl. Akad. Nauk SSSR* **149** 1311 (1963).
25. ——— and P. H. Roberts, *Geophys. Astrophys. Fluid Dyn.* **79**, 1 (1995)
26. B. A. Buffett, H. E. Huppert, J. R. Lister, A. W. Woods, *J. Geophys. Res.* **101**, 7989 (1996).
27. N. H. Sleep, *J. Geophys. Res.* **95**, 6715 (1990); D. E. Loper, *Geomagn. Geoelect.* **43**, 79 (1991).
28. D. E. Loper, *J. Geophys. Res.* **83**, 5961 (1978).
29. S. Labrosse, J. P. Poirier, J. L. LeMouel, *Phys. Earth Planet. Inter.* **99**, 1 (1997); J. R. Lister and B. A. Buffett, *Phys. Earth Planet. Inter.* **105**, 5 (1998).
30. D. E. Loper, *Geophys. J. R. Astron. Soc.* **54**, 389 (1978).
31. J. R. Lister and B. A. Buffett, *Phys. Earth Planet. Inter.* **91**, 17 (1995).
32. D. J. Stevenson, T. Spohn, G. Schubert, *Icarus* **54**, 466 (1983).
33. T. N. W. McElhinney and W. E. Senanayake, *J. Geophys. Res.* **85**, 3523 (1980).
34. The characteristic time τ for ohmic decay of the magnetic field in the absence of fluid motions is $\tau = L^2/\pi^2\,\eta$, where L is the characteristic length scale for the magnetic field and η is the magnetic diffusivity. The radius of the core is a representative length scale, so we let $L = 3 \times 10^6$ m and $\eta = 2$ m^2 s^{-1}. This gives $\tau = 1.5 \times 10^4$ years.
35. P. Olson and G. A. Glatzmaier, *Phys. Earth Planet. Inter.* **92**, 109 (1995).
36. Recent reviews of the geodynamo are given by R. Hollerbach [*Phys. Earth Planet. Inter.* **98**, 163 (1996)], D. R. Fearn [*Rep. Prog. Phys.* **61**, 175 (1998)], and F. H. Busse [*Annu. Rev. Fluid Mech.* **32**, 383 (2000)].
37. A recent review of the work of G. I. Taylor by M. P. Brenner and H. A. Stone [*Physics Today* **53**, 30 (2000)] includes a photograph that clearly demonstrates the columnar pattern of flow in a rapidly rotating fluid. The photograph is taken from the study of J. W. M. Bush, H. A. Stone, and J. Bloxham [*J. Fluid Mech.* **282**, 247 (1995)].
38. N. A. Phillips, *Rev. Geophys.* **1**, 123 (1963).
39. The dynamical state of the core may be approximated by a geostrophic balance that is disturbed by the addition of buoyancy forces, as well as magnetic and viscous forces. From the radial component of the curl of the leading-order force balance, we find that radial flow is not possible unless the magnetic and/or viscous forces are present.
40. Convection in a rapidly rotating fluid with no magnetic forces takes the form of narrow rolls that align with the rotation axis. The aspect ratio of the rolls is about $E^{1/3}$ to 1, where $E \approx 10^{-15}$ is the Ekman number [P. H. Roberts, *Philos. Trans. R. Soc. London A* **263**, 93 (1963)].
41. The importance of the Lorentz force in the force balance is measured relative to the Coriolis force. These two forces become comparable when the magnetic field is nominally 10^{-3} T.
42. K. Zhang and D. Gubbins, *Geophys. J. Int.* **140**, F1 (2000).
43. C. G. Langereis *et al.*, *Geophys. J. Int.* **129**, 75 (1997).
44. S. I. Braginsky and V. P. Meytlis, *Geophys. Astrophys. Fluid Dyn.* **55**, 71 (1990).
45. D. R. Fearn, M. R. E. Proctor, C. C. Sellars, *Geophys. Astrophys. Fluid Dyn.* **77**, 111 (1994).
46. G. A Glatzmaier and P. H. Roberts, *Physica D* **97**, 81 (1996).
47. J. M. Aurnou, D. Brito, P. Olson, *Geophys. Res. Lett.* **23**, 3401 (1996).
48. G. A. Glatzmaier and P. H. Roberts, *Science* **274**, 1887 (1996).
49. B. A. Buffett and G. A. Glatzmaier, in preparation.
50. K. Zhang and C. A. Jones, *Geophys. Res. Lett.* **24**, 2869 (1997); ———, G. R. Sarson, *Stud. Geophys. Geod.* **42**, 247 (1998).
51. U. Christensen, P. Olson, G. A. Glatzmaier, *Geophys. Res. Lett.* **25**, 1565 (1998).
52. D. Gubbins and J. Bloxham, *Nature* **325**, 509 (1987).
53. R. T. Merrill and P. L. McFadden, *Rev. Geophys.* **37**, 201 (1999).
54. A. Cox, *Rev. Geophys.* **13**, 35 (1975).
55. D. Jault, G. Hulot, J. L. LeMouel, *Phys. Earth Planet. Inter.* **98**, 1987 (1996); S. Zatman and J. Bloxham, *Nature* **388**, 760 (1997).
56. P. Kelly and D. Gubbins, *Geophys. J. Int.* **128**, 315 (1997); C. L. Johnson and C. G. Constable, *Geophys. J. Int.* **131**, 643 (1997).
57. T. Lay, Q. Williams, E. J. Garnero, *Nature* **392**, 461 (1998).
58. J. Bloxham and D. Gubbins, *Nature* **325**, 511 (1987).
59. K. Zhang and D. Gubbins, *Phys. Fluids* **8**, 1141 (1996); G. R. Sarson, C. A. Jones, A. W. Longbottom, *Phys. Earth Planet. Inter.* **101**, 13 (1997).
60. P. Olson and G. A. Glatzmaier, *Philos. Trans. R. Soc. London A* **354**, 1413 (1996).
61. I. Sumita and P. Olson, *Science* **286**, 1547 (1999).
62. G. A. Glatzmaier, R. Coe, L. Hongre, P. H. Roberts, *Nature* **401**, 885 (1999).
63. J. Bloxham, *Philos. Trans. R. Soc. London A* **358**, 1171 (2000).
64. ———, *Nature* **405**, 63 (2000).
65. R. Jeanloz, *Annu. Rev. Earth Planet. Sci.* **18**, 357 (1990); E. Knittle and R. Jeanloz, *Science* **251** 1438 (1991).
66. F. H. Busse and J. Wicht, *Geophys. Astrophys. Fluid Dyn.* **64**, 135 (1992)
67. B. A. Buffett, *Geophys. J. Int.* **125**, 303 (1996).
68. R. Holme, *Phys. Earth Planet. Inter.* **117**, 329 (2000).
69. M. Manga and R. Jeanloz, *Geophys. Res. Lett.* **23**, 3091 (1996).
70. D. Jault and J. L. LeMouel, *Geophys. Astrophys. Fluid Dyn.* **48**, 273 (1989); B. A. Buffett, *Geophys. Res. Lett.* **23**, 2279 (1996).
71. R. Hide, *Science* **157**, 55 (1967).
72. A. Morelli, A. M. Dziewonski, J. H. Woodhouse, *Geophys. Res. Lett.* **13**, 1545 (1986).
73. A review of elastic anisotropy in the inner core is given by X. D. Song [*Rev. Geophys.* **35**, 297 (1997)].
74. S. Tanaka and H. Hamaguchi, *J. Geophys. Res.* **102**, 2925 (1997); K. C. Creager, *J. Geophys. Res.* **104**, 23137 (1999); J. E. Vidale and P. S. Earle, *Nature* **404**, 273 (2000).
75. T. J. McSweeney, K. C. Creager, R. T. Merrill, *Phys. Earth Planet. Inter.* **101**, 131 (1997); X. D. Song and D. V. Helmberger, *Science* **282**, 924 (1998).
76. L. Stixrude and R. E. Cohen, *Science* **267**, 1972 (1995); G. Steinle-Neumann, L. Stixrude, R. E. Cohen, *Phys. Rev. B* **60**, 791 (1999).
77. S. C. Singh, M. A. J. Taylor, J. P. Montagner, *Science* **287**, 2471 (2000).
78. I. Sumita, S. Yoshida, M. Kumazawa, Y. Hamano, *Geophys. J. Int.* **124**, 502 (1996).
79. R. Jeanloz and H. R. Wenk, *Geophys. Res. Lett.* **15**, 72 (1988); S. Karato, *Science* **262**, 1708 (1993); S. Yoshida, I. Sumita, M. Kumazawa, *J. Geophys. Res.* **101**, 28085 (1996); M. I. Bergman, *Nature* **389**, 60 (1997); S. Karato, *Nature* **402**, 871 (1999).
80. A summary of proposed explanations for elastic anisotropy in the inner core is given by B. A. Buffett in *Mineral Physics and Seismic Tomography*, S. Karato *et al.*, Eds. (American Geophysical Union, Washington, DC, 2000).
81. X. D. Song and P. G. Richards, *Nature* **382**, 221 (1996); W. J. Su, A. M. Diewonski, R. Jeanloz, *Science* **274**, 1883 (1996).
82. W. J. Su and A. M Dziewonski, *J. Geophys. Res.* **100**, 9831 (1995).
83. K. C. Creager, *Science* **278**, 1284 (1997).
84. A. Souriau, *Geophys. J. Int.* **134**, F1 (1998); ——— and G. Poupinet, *Phys. Earth Planet. Inter.* **118**, 13 (2000).
85. D. S. Sharrock and J. H. Woodhouse, *Earth Planets Space* **50**, 1013 (1998); G. Laske and G. Masters, *Nature* **402**, 66 (1999).
86. B. A. Buffett, *Geophys. Res. Lett.* **23**, 3803 (1996); *Nature* **388**, 571 (1997).
87. X. D Song, *J. Geophys. Res.* **105**, 623 (2000).

88. This review was written during a visit to the Berkeley Seismological Laboratory at the University of California. I thank B. Romanowicz and the staff of the Seismological Laboratory for their hospitality. J. Bloxham, G. Glatzmaier, and P. Olson kindly provided figures from their work. R. Jeanloz and S. Zatman offered many helpful suggestions on the manuscript. Supported by a Killiam Faculty Research Fellowship.